NANOFLUIDIC DEVICE ARCHITECTURES FOR THE CONTROLLED TRANSPORT AND HIGH THROUGHPUT ANALYSIS OF SINGLE DNA MOLECULES IN NANOCHANNELS

L.D. Menard and J.M. Ramsey*

Department of Chemistry, University of North Carolina at Chapel Hill, USA

ABSTRACT

Devices with intersecting nanofluidic elements were developed to control the transport of DNA molecules through nanochannels. Independent voltage inputs decoupled translocation event frequency from transport velocity, facilitating the imaging-based analysis of many DNA molecules. In one application, we measured the extension length of a single molecule in a series of nanochannels with diameters ranging from 175 to 500 nm. DNA extension, R, scales with nanochannel diameter, D: $R \sim D^{\alpha}$. We found a value for the exponent, α=0.71±0.03, in agreement with theory (α=0.70) [1] but in contrast to a previous result (α=0.85±0.05) [2] from measurements collected across multiple devices.

KEYWORDS: Nanochannels, Nanofluidics, DNA, Single-Molecule, Confinement, Extension

INTRODUCTION

The direct reading of genomic maps from chromosomal DNA is facilitated by the linearization and extension of DNA molecules [3]. Homogenous extension can be achieved by forcing DNA molecules into fluidic channels having diameters less than a few hundred nanometers. Fluorescently stained molecules are imaged in their extended state after introduction to these nanochannels or during their driven transport through a nanochannel [4, 5]. In this latter, continuous-flow mode of operation, DNA molecules can also be monitored using single-point detection [6, 7]. In either case, the precise control of DNA transport into and through nanofluidic channels will improve device performance with regard to throughput, sampling efficiency, and the uniformity of extension. The presented devices achieve such control through the use of multiple intersecting nanochannels that are independently voltage controlled. This extension of microfluidic control schemes requires a consideration of phenomena that are unique to the nanoscale.

THEORY

Two primary theories describe the extension of long DNA molecules confined in nanochannels: the blob model of de Gennes [8] and the reflecting rod model of Odijk [9]. These theories are appropriate when the confining dimensions are greater than or less than the DNA persistence length, respectively. The persistence length, a measure of the molecule's bending stiffness, is ~50 nm for double-stranded DNA in high ionic strength solutions. Recent theoretical work and simulations of confined DNA molecules have resulted in refinements to these models, specifically in describing the transition between the two regimes [1]. In de Gennes' theory, the extension length, R, of DNA molecules in nanochannels larger than DNA's persistence length, P, is expected to vary with the channel diameter, D, according to the following relationship [8]:

$$R = LD^{-2/3}(Pw)^{1/3} \tag{1}$$

where L is the molecule's contour length and w its width. Using a more exact value of the Flory exponent ($\nu = 0.5877$), the dependence of extension length on channel diameter is expected to scale as $D^{-0.70}$ [1]. Previously reported experimental results, however, found a power law dependence of $D^{-0.85}$ [2, 10].

The electrophoretically driven introduction of a DNA molecule into a nanochannel subjects the molecule to considerable stress. When a molecule is pulled into a nanochannel, the force induced by the high field strength is opposed by the drag of the molecule's trailing end. This was found to cause significant extension of the DNA molecule when it is pulled into the nanochannel [11]. For worm-like chains the force-extension relationship was approximated by Marko and Siggia using the following equation [12]:

$$F = \frac{k_B T}{P}\left[\frac{1}{4(1-x/L)^2} - \frac{1}{4} + \frac{x}{L}\right] \tag{2}$$

where k_B is Boltzmann's constant, T is temperature, and x is the force-induced extension. We note that the force applied to a molecule scales with the number of DNA monomers in the high-field region (*i.e.*, in the nanochannel) and thus with the DNA contour length. It is desirable to control the forces acting on long DNA molecules in order to prevent shearing.

EXPERIMENTAL

Devices were fabricated in fused quartz substrates. Microfluidic channels were patterned using photolithography and wet etching. The nanofluidic components consisted of two types of conduits: nanochannels and nanoslits. Nanochannels having square cross-sectional profiles with widths and depths ranging from 15 to 500 nm were fabricated using focused ion beam milling [13]. Nanoslits with widths ≥1 μm were patterned into a resist layer using either electron beam

lithography or photolithography, followed by transfer of the pattern into the substrate by wet etching to a depth of 2-10 nm. Nanochannels served as the conduits of DNA transport while nanoslits were used as orthogonal interconnects in a crossed-channel geometry that enabled precise voltage control (Fig. 1). The use of shallow features inhibited DNA transport into these auxiliary conduits due to an entropic barrier to increased DNA confinement. The fluidic network was sealed by thermal bonding of a fused quartz coverslip to the substrate.

Double-stranded phage DNA molecules (λ-phage, 48.5 kbp; T4-phage, 165.6 kbp) were stained with the intercalating dye YOYO-1 in Tris-borate-EDTA (TBE) electrophoresis buffers. DNA molecules were electrophoretically driven through the transport nanochannel by applying voltages across each of the four fluidic elements shown in Figure 1. The voltage at the channel intersection was tuned to control the relative field strengths of the high- and low-field segments of the transport nanochannel. Experiments were conducted on an inverted fluorescence microscope using a 100X oil immersion objective. Fluorescence was excited using illumination from a mercury arc lamp filtered through a 472-nm excitation filter and detected through a 520-nm emission filter with imaging by an em-CCD camera.

RESULTS AND DISCUSSION

The ability to generate a high electric field at the entrance of the transport nanochannel and a significant field strength in the microchannel supplying DNA molecules ensures a high frequency of transport events. The transport of DNA molecules through the nanochannel's high-field segment occurs too rapidly to accurately image the process given the sensitivity and bandwidth limitations of CCD or CMOS cameras. With the passage of DNA molecules into the low-field segment of the nanochannel, however, the transport velocity decreases over 100 fold (Fig. 2), enabling high signal-to-noise imaging without blurring during continuous flow operation. We note that very long DNA molecules can be pulled into the transport nanochannel by the strong field at the channel entrance but that the total force acting on the molecule can be minimized by limiting the length of this segment (*e.g.*, <20 μm long). This approach minimizes DNA shearing.

The applied voltages can also be adjusted to induce stable trapping at the nanochannel intersection, followed by the actively controlled release and further manipulation of a DNA molecule. This strategy was used to introduce single DNA molecules into a series of nanochannels with a range of diameters (Fig. 3a). A molecule was successively moved to the center of each of the nanochannels then allowed to equilibrate for at least 1 min after the voltages were zeroed. The molecule was then imaged for 30 s following the equilibration period (Fig. 3b). Plots of the equilibrium extension length for each molecule as a function of channel diameter were then individually fit to a power law (Fig. 3c). This approach eliminates errors that might arise from sampling over different sub-populations of molecules with variable size.

We found that concentration polarization affected transport behavior in devices having very shallow nanoslits (<5 nm deep) using low ionic strength buffers. This phenomenon was found to be advantageous for effectively trapping DNA molecules at the nanochannel intersection but inhibited smooth continuous flow operation such as that shown in Figure 2.

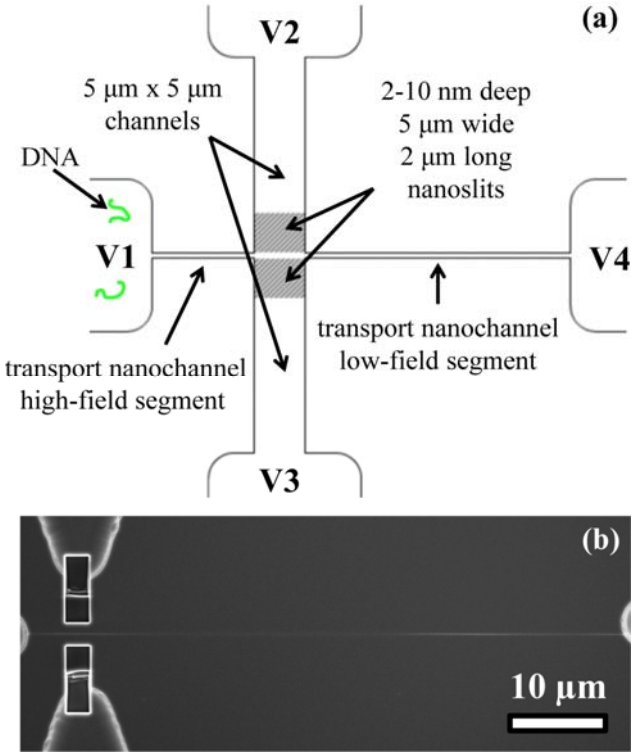

Figure 1: (a) Schematic of a device with intersecting nanofluidic elements. (b) Scanning electron microscope (SEM) image of a representative device. The nanoslits are not visible in this top-down view.

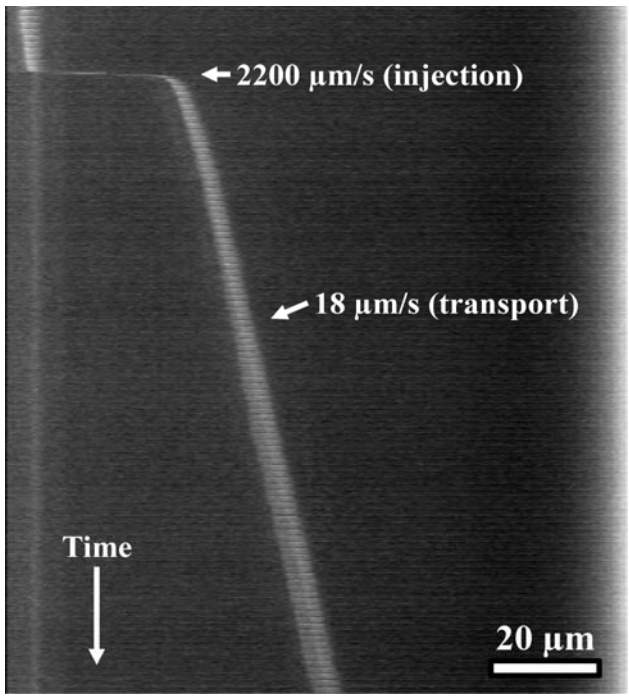

Figure 2: Series of frames from a movie (stacked vertically) showing the fast injection of λ-phage DNA into a 100-nm transport channel. The DNA velocity slows 120 fold as the molecule passes through the intersection of the device. 0.5x TBE electrophoresis buffer. V1=0 V; V2,V3,V4=4 V. 250 frames/s.

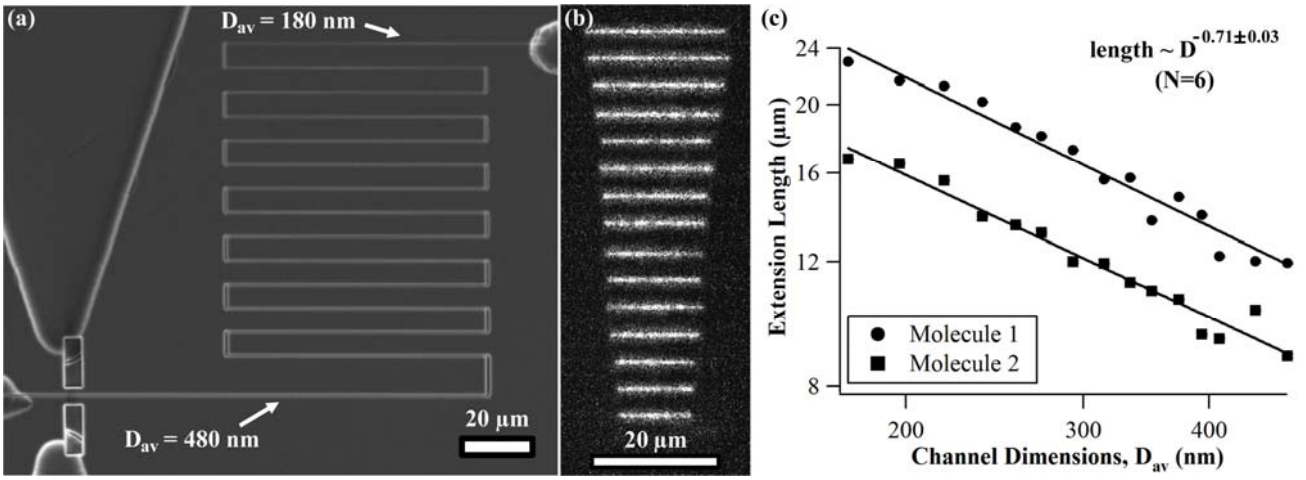

Figure 3: (a) SEM image of a device having a series of nanochannels with decreasing diameters. A single T4-phage DNA molecule can be introduced to the nanochannels, imaged after equilibration in each segment, and then driven to the next segment. (b) Representative fluorescence images of the same DNA molecule in each segment. (c) Extension lengths as a function of channel dimensions for two molecules. Their difference in length reflects the distribution of sizes in a sample of phage DNA due to shearing during extraction or sample handling. Error bars, representing the standard error of each measurement, are smaller than the data symbols.

CONCLUSION

We demonstrated the use of intersecting nanofluidic channels and slits to actively control the dynamics of DNA transport through nanochannel devices. The presented devices offer a significant improvement in the number of molecules that can be precisely characterized in fluidic nanochannels. Device performance is impacted by nanoscale phenomena such as concentration polarization and conformational entropy barriers. Future work will demonstrate the advantages of these devices for introducing long (>500 Mbp) DNA molecules into nanochannels without shearing.

ACKNOWLEDGEMENTS

This work was sponsored in part by a grant from the National Human Genome Research Institute, National Institutes of Health (Grant R01HG02647-05).

REFERENCES

[1] Y. Wang, D. R. Tree, K. D. Dorfman, *Macromolecules* 44, 6594-6604 (2011).
[2] W. Reisner, K. J. Morton, R. Riehn, Y. M. Wang, Z. Yu, M. Rosen, J. C. Sturm, S. Y. Chou, E. Frey, R. H. Austin, *Phys. Rev. Lett.* 94, 196101 (2005).
[3] M. Levy-Sakin and Y. Ebenstein, *Curr. Opin. Biotech.* in press, DOI:10.1016/j.copbio.2013.01.009
[4] L. D. Menard and J. M. Ramsey, *Anal. Chem.* 85, 1146-1153 (2013).
[5] W. Reisner, J. N. Pedersen, R. H. Austin, *Rep. Prog. Phys.* 75, 106601 (2012).
[6] L. D. Menard, C. E. Mair, M. E. Woodson, J. P. Alarie, J. M. Ramsey, *ACS Nano* 6, 9087-9094 (2012).
[7] C. H. Reccius, S. M. Stavis, J. T. Mannion, L. P. Walker, H. G. Craighead, *Biophys. J.* 95, 273-286 (2008).
[8] J. Daoud and P. G. de Gennes, *J. Phys. (Paris)* 38, 85-93 (1977).
[9] T. Odijk, *Macromolecules* 16, 1340-1344 (1983).
[10] F. Persson, P. Utko, W. Reisner, N. B. Larsen, A. Kristensen, *Nano Lett.* 9, 1382-1385 (2009).
[11] L. D. Menard, J. S. Zhou, M. E. Woodson, C. E. Mair, J. P. Alarie, J. M. Ramsey, *µTAS 2011*, pp. 1761-1763.
[12] J. F. Marko and E. D. Siggia, *Macromolecules* 28, 8759-8770 (1995).
[13] L. D. Menard and J. M. Ramsey, Nano Lett. 11, 512-517 (2011).

CONTACT

*J. M. Ramsey, Tel: +1-919-962-7492; jmramsey@unc.edu